MASTER'S THESIS

INVESTIGATION OF PROTON INDUCED REACTIONS IN LIGHT NUCLEI USING PROPORTIONAL COUNTER

CAPTAIN J. O. F. DORSETT, USN
THE OHIO STATE UNIVERSITY

1952

THESIS
D66

Thesis
D66

INVESTIGATION OF PROTON INDUCED REACTIONS IN LIGHT NUCLEI USING PROPORTIONAL COUNTER

Abstract of

A Thesis

Presented in Partial Fulfillment of the Requirements
for the Degree Master of Science

By

JOHN OREM FILLMORE DORSETT, B.S., M.S. (Met.)

The Ohio State University

1952

Approved by:

Adviser

Library
U. [illegible] duate School
Monterey, California

Thesis
D66

INVESTIGATION OF PROTON INDUCED REACTIONS IN LIGHT NUCLEI USING PROPORTIONAL COUNTER

John Orem Fillmore Dorsett
B. S., U.S. Naval Academy, 1937
M. S., (Met.) Massachusetts Institute of Technology, 1940

Department of Physics
(Approved by James C. Harris)

The general problem was to utilize a proportional counter for observing nuclear reactions induced in proton bombardments by The Ohio State University Van de Graaff electrostatic generator.

The proportional counter, designed by Commander A. B. Chilton, was modified and improved by the addition of a reaction collimator and electrostatic shield between the sensitive volume and reaction chamber. The particular problem investigated was the elastic scattering of protons by argon gas. The gaseous target and filling gas of the counter were the same: 90% argon and 10% CO_2 under 50 mm. (Hg) pressure. Scattering angle in the laboratory system was 150°. A proton beam current of about 0.2 - 0.3 microamperes was integrated in cycles of 10.9 microcoulombs. or about 6000 counts per minute.

Elastic scattering rate was investigated for proton

reaction energies from 710 to 1133 kev. The general trend followed closely the predicted scattering obtained by adding the cross-sections due to Coulomb potential and that due to a hard sphere type of scattering. A definite anomaly was observed at 908 ± 10 kev. Since the experimental resolution was of the order of 20 kev., no attempt was made to compute the resonance width from the energy spread of the extrema. A second run confirmed the existence and shape of the anomaly. The energy of this resonance in K^{41} agrees closely with investigations made by Broström, Huus, and Koch in 1948 (Nature <u>162</u>, 695.)

INVESTIGATION OF PROTON INDUCED REACTIONS IN LIGHT NUCLEI USING PROPORTIONAL COUNTER

A Thesis
Presented in Partial Fulfillment of the Requirements
for the Degree Master of Science

By

JOHN [illegible] FILLMORE [illegible], B.S., M.S. (Met.)

The Ohio State University

1952

Approved by:

Adviser

ACKNOWLEDGMENTS

To Dr. James C. Harris particular thanks are due for suggesting the problem and for his continual advice and encouragement through the trials of getting all apparati to funtion smoothly and simultaneously. I wish to thank Commander Arthur B. Chilton for his original design and construction of the proportional counter and his advice in operating the equipment, and Dr. John N. Cooper for his words of encouragement, his interest in the problem, and advice in operation of the Van de Graaff generator. Finally, I would like to thank Messrs. Ottis Campbell and Ignas Saldukas for technical assistance in operation of the Van de Graaff.

This work was carried out under the auspices of the United States Naval Postgraduate School at Monterey, California.

TABLE OF CONTENTS

I. GENERAL

The problem in general was to investigate certain proton induced reactions using a sensitive and highly discriminating proportional counter. The Van de Graaff generator at The Ohio State University provides a source of protons of fairly discrete energies within the range of 0.3 and 1.5 Mev. The reactions induced in targets made of various materials were to be detected by means of a sensitive proportional counter. When used with a linear amplifier having a discriminating circuit, a method was provided for detecting and discriminating between proton groups or between protons and alpha particles.

Originally, it was planned to investigate the ($p-\alpha$) reactions in light nuclei using as a target very thin nickel or copper foil. Difficulties were encountered in monitoring the beam with a solid target installed, especially since the beam current had to be kept down to the order of 0.1 microampere to avoid saturating the counter with recoil protons. Suggestions for correcting this difficulty are discussed in Section VI. Pending further modification of the target assembly, it was decided to investigate elastic scattering from the argon used as a counting gas in the chamber. This type of experiment per-

mitted visual monitoring of the beam while using low beam currents.

Two possibilities were recognized: (1) anomolies in the elastic scattering would indicate resonances in A and (2) a low energy (p-α) reaction is energetically possible from atomic mass considerations with $Q = +1.64$ Mev. The chance that the latter reaction might have a large cross-section was deemed to be very remote because of the high Coulomb barrier of argon to both incident and emitted particles. The reaction is as follows:

$$_{18}A^{40} + {}_{1}H^{1} = \left({}_{19}K^{41}\right)^{*} = {}_{17}Cl^{37} + {}_{2}He^{4} + Q \ (= 1.64 \text{ Mev.})$$

The (p-n) reaction for A^{40} was ruled out on account of a negative Q of approximately -1.7 Mev.

II. HISTORICAL AND BACKGROUND

Scattering phenomena belong to one of three general classes:

(1) Elastic (Coulomb or Rutherford) scattering.

(2) Inelastic scattering.

(3) Resonance scattering.

Elastic Scattering.

Elastic scattering occurs when the kinetic energy of the system is conserved. In the case of a fast light particle "colliding" with a heavy slow moving particle the light particle has almost the same energy after collision as before. Rutherford's original theory of the atomic nucleus was verified by experiments in which the elastic scattering of α-particles from thin gold foils was observed. He assumed that the positive charge of the gold nucleus was concentrated in a small volume which contained most of the atomic mass. This charge was considered as a point charge whose electric field satisfied the Coulomb Law of Repulsion. The exact deflection of small positive charges such as Alphas would depend on the initial path of the particle with respect to the bombarded nucleus. Elastic scattering will be covered in greater detail in the next section.

Inelastic Scattering.

If the incident particle penetrates within the Coulomb barrier so that the short range nuclear forces come into

play, kinetic energy and momentum will not be separately conserved. Some of the particle energy is transferred to the nucleus which goes to an excited quantum state. The transferred energy is emitted as a gamma photon when the nucleus, after emitting a particle of the same kind as the incident particle, returns to the ground state again. Such a process is inelastic scattering. The problem of inelastic scattering has been treated by Born[1] as a perturbation problem in quantum mechanics.

Inelastic scattering of protons has been investigated by several workers: Dicke and Marshall (1945)[2]; Wilkins (1941)[3]; Davis and Haffner (1948)[4]; Powell, May, Chadwick and Pickavance (1940)[5]; Fulbright and Bush (1948)[6]; and Thoderick (1950)[7].

Whereas, elastically scattered charged particles are scattered mainly in the forward direction, inelastically scattered particles tend to a symmetrical angular distribution. This indicates the formation of a compound nucleus from which the entering particle is re-emitted with spherical symmetry.

Inelastic scattering of protons may be thought of as a (p,p) reaction in which the proton leaves with a lower kinetic energy. The scattering nucleus is raised to an excited state at the expense of the kinetic energy of the system. Observation of the energy spectrum of the scattered protons

gives information of the nuclear levels involved. Before interpretation can be made of the results, the possibility of such a reaction as that shown in Fig. 1(b) must be excluded.[7]

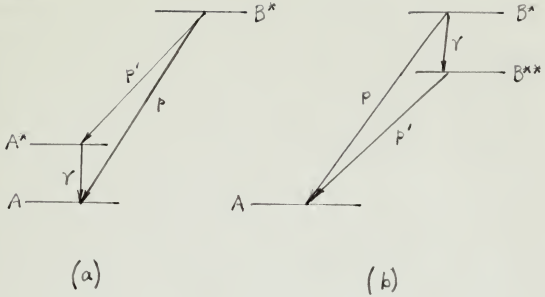

Fig. 1.

The process diagrammed in Fig. 1(b) produces inelastically scattered protons but does not involve any excited states of the residual nucleus. Rhoderick[7] states that the probability at most of such a process taking place is only one-thousandth as great as that of a direct transition to the ground state of B. This is far less probable than simple capture, which in turn is far less likely than emission of a proton, because of the smallness of the radiative width of nuclear levels. We can therefore assume that inelastic scattering follows the pattern of

Fig. 1(a), and therefore the loss of energy of the proton (in the center-of-mass system) is equal to the excitation energy of the residual nucleus.

Dicke and Marshall[2] point out that (p,n) reactions are much more likely than (p,p) reactions due to the Coulomb barrier. Thus, if the (p,n) reaction is energetically possible, one would expect very little (p,p) inelastic reactions. Substances most suitable for inelastic proton scattering are those with high (p,n) thresholds and these are found mostly in light nuclei.

Powell, et al[5], obtained information on probability of scattering at angles of 15° through 150°. Inelastically scattered protons from neon were found to be distributed with spherical symmetry. No inelastic protons were observed in oxygen up to 4 Mev. Chlorine and argon were investigated and the ratio of inelastic to elastic scattering was very much smaller than in the case of neon corresponding to the decreased probability of protons entering the nucleus with increasing nuclear charge.

When the bombarding particle penetrates the nuclear barrier to form a compound nucleus, the scattering ceases to be purely elastic and becomes a *transmutation process*. Historically, the first of these processes[8] was Rutherford's bombardment of nitrogen in 1919 with alpha particles to form oxygen in the ground state with the emission of a proton. The equation for this reaction is:

$N^{14} + {}_{2}He^{4} = ({}_{9}F^{19})^{*} = {}_{8}O^{17} + {}_{1}H^{1} + Q$ (= -1.26 Mev.)

The first successful disintegration utilizing protons was performed by Crockcroft and Walton in 1932.[9] Protons were accelerated in a hydrogen discharge tube up to 0.5 Mev. and used to bombard lithium; alpha particles were observed on a fluorescent screen. The reaction[10,11] is:

${}_{3}Li^{7} + {}_{1}H^{1} = ({}_{4}Be^{8})^{*} = {}_{2}He^{4} + {}_{2}He^{4} + Q$ (+17.13 Mev.)

This reaction has now been studied by many observers and is so well known as to be a calibrating reaction.

Other important (p-α) reactions summarized by Livingston and Bethe in Rev. Mod. Phys. 9, 311 (1937) were reported by: Neuert[11]; Kirchner and Neuert[12]; Oliphant, Kempton, and Rutherford[13]; Dee and Gilbert[14]; and Henderson, Livingston, and Lawrence[15].

Resonance Phenomena

At certain proton energies the probability that the excitation energy of the compound nucleus is close to one of the quantum states is high. The probability of the formation of the compound nucleus, therefore is great. Such a condition is called resonance. It corresponds to the excitation of a mechanical system when an impressed force oscillates with a frequency near the mechanical resonant frequency.[16]

Resonances may be observed in several ways. One way is

to note the disappearance of incident particles, that is, a peak in the cross-section for capture. Another method is to look for increased effects associated with the formation of a compound nucleus. These would be a peak in either gamma emission or production of some other particle than the incident particle such as the (p-α), (d-α), (p-n), (n-p), etc. Still another method is to observe anomalies in the elastic scattering of protons of which more will be said in the next section.

If gamma rays only are observed, I.e. heavy particle emission is impossible, the quantum (or excited) state is called a *bound* state. If particles can be emitted (p, α, or n) however, the state is called a *virtual* state. Energy levels in light nuclides are beginning to be fairly well known and have been reviewed and summarized by various writers.[17,18]

Devons[19] states that observation of discrete resonances in nuclei of $Z > 30$ is not likely since the proton energy for appreciable yields (~3 Mev.) corresponds to an excitation energy of the compound nucleus in excess of 10 Mev. at which energies the level spacing of quantum states is probably less than any energy resolution experimentally attainable.

The mean life of an excited state is related to the level width by the uncertainty relation:

$$\Gamma \cdot \tau = \frac{h}{2\pi}$$

where
Γ = level width
τ = mean life
h = Planck's constant

This says that well defined states have long lifetimes, and

conversely. With the high excitations necessary for heavy nuclides, the levels become wider than the mean interval between neighboring levels. Proton resonances have been observed only for nuclei of Z up to 20, the processes observed were (p,γ), (p,α) and elastic scattering.

Freeman and Baxter[20] found (p,α) resonances in Na^{23} at proton energies of 590, 750, 800, and 910 Kev. with Q = 2.14 Mev. and Al^{27} at proton energies of 650,730, and 920 Kev. with Q = 1.32 Mev.

Resonances in K^{41} due to proton bombardment of A^{40} have been reported by Broström, Huus, and Koch[21] as follows:

E_p (Kev.)	900	1050	1080	1100	1235
$y - y_0$	0.2	0.4	0.5	1.0	0.5

where $y - y_0$ = difference between resonance yield, y, in counts/μC. and background, y_0, which was about 0.1 for all resonances.

Proton scattering experiments using the Van de Graaff generator as a source provides a means for initiating resonance phenomena. Observation of these furnishes information on the excited states of the compound nucleus. Some of the results obtainable from the study of resonance peaks are:

(1) Energy of excited states,

(2) Mean life of excited states,

(3) Interference between excited states, and

(4) Modes of decay of excited states.

III. THE ELASTIC SCATTERING PROBLEM.

As stated in Section II, elastic scattering occurs when the kinetic energy of the system is conserved. For a pure Coulomb potential, $V(r) \sim \frac{1}{r}$, Rutherford derived from purely classical considerations a formula for the differential cross-section:

$$\sigma_c(\theta) = \left[\frac{zZe^2}{4E}\right]^2 \frac{1}{\sin^4\left(\frac{\theta}{2}\right)}$$

where θ = scattering angle (deviation)
e = electronic charge
z = atomic no. of incident particle
Z = atomic no. of scattering nucleus
E = kinetic energy of incident particle

Being a long range type of potential, $\sigma_c(\theta)$ is strongly dependent on the angle of scattering. Figure 2 is a plot of the factor: $\frac{1}{\sin^4\left(\frac{\theta}{2}\right)}$ showing that Coulomb (Rutherford) scattering is mostly in the forward direction.

Landé [22] treats the problem from a wave mechanical point of view where a modified Coulomb potential[23] is considered as a perturbation.

The modified potential is: $U'(r) = \frac{zZe^2}{r} \exp\left(-\frac{r}{r_0}\right)$ where where r_0 is a parameter which limits the Coulomb force. Such a modified potential actually exists for charged particles scattered by neutral atoms. The solution of this

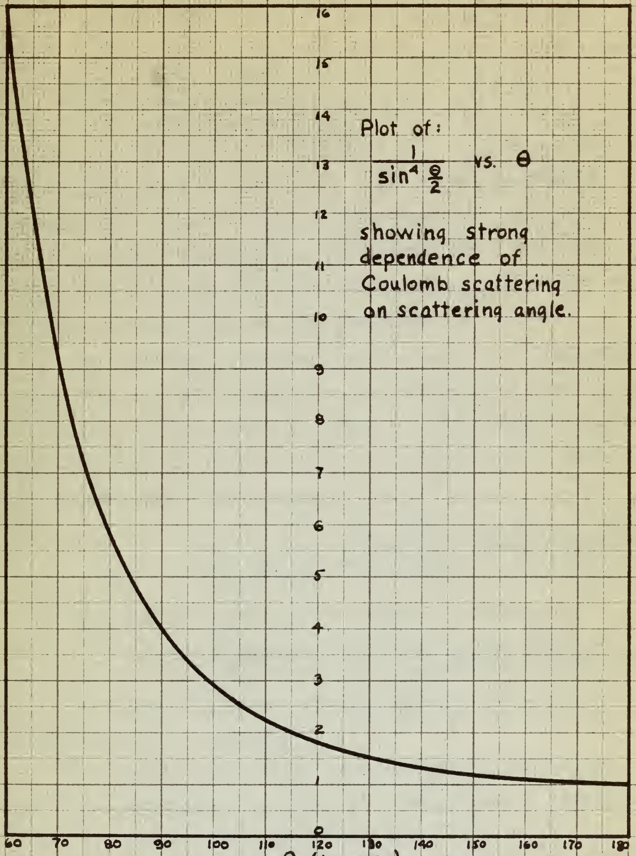
16
15
14
13
12
11
10
9
8
7
6
5
4
3
2
1
0
Plot of:
$\frac{1}{\sin^4 \frac{\theta}{2}}$ vs. θ
showing strong dependence of Coulomb scattering on scattering angle.
60
70
80
90
100
110
120
130
140
150
160
170
180
θ (degrees)

FIGURE 2

yields a cross-section which has a finite value at $\theta = 0$, viz.,

$$\sigma_c(\theta) = \left[\frac{zZe^2}{4E\sin^2\frac{\theta}{2} + \left(\frac{\hbar}{2mv_0 r_0}\right)^2}\right]^2$$

When $r_0 = \infty$, the formula is the same as the Rutherford formula, but for finite r_0, $\sigma_c(\theta)$ remains finite at $\theta = 0$.

The above formulae apply for scattering of protons by large nuclei but not for proton-proton scattering due to the "exchange" forces between like particles.

The differential cross-section is a ratio of the number of particles scattered per unit solid angle (steradian) in the direction θ to the number of incident particles per unit area. The number of particles per unit solid angle, $n(\theta)$, scattered in the direction θ is therefore:

$n(\theta) = n_0 N t \sigma_c(\theta)$ [This assumes that multiple scattering is small and that the scattering centers do not shield one another.]

where n_0 = initial no. of incident particles

N = no. of scattering atoms per unit volume

t = thickness of scattering medium (linear units)

In estimating cross-section for elastic scattering three factors must be considered:

(1) Modification of the incident beam by the Coulomb field before reaching the nuclear forces. (Rutherford scattering.)

(2) Potential scattering by a specifically nuclear field

of force.

(3) Scattering in which a compound nucleus is formed.

Using the Rutherford formula and assuming our detecting apparatus counts scattered protons at a constant angle, θ_0, from the incident beam, we can plot the no. of scattered protons as functions of beam energy. Using arbitrary units for counting rate of 100 protons/sec. at an energy of 1 Mev. the relation is:

$$n(E) = \frac{100}{E^2} \quad (\text{protons/sec.})$$

This curve is plotted in Figure 3.

Anomalies or deviations from the counting rate predicted by the Rutherford formula will be found for certain energies of the incident particle depending on factors (2) and (3) above. If the energy of the incident proton plus the energy of the scattering nucleus is equal to the energy of one of the quantum states of the compound nucleus, anomalous scattering will occur. Siri[24] states that anomalous scattering that increases slowly with increasing particle energy indicates penetration of the nuclear barrier; and anomalous scattering that increases rapidly to a maximum and then decreases as the energy is further increased indicates resonance scattering.

Resonance Scattering.

In order to see what these anomalies in Rutherford

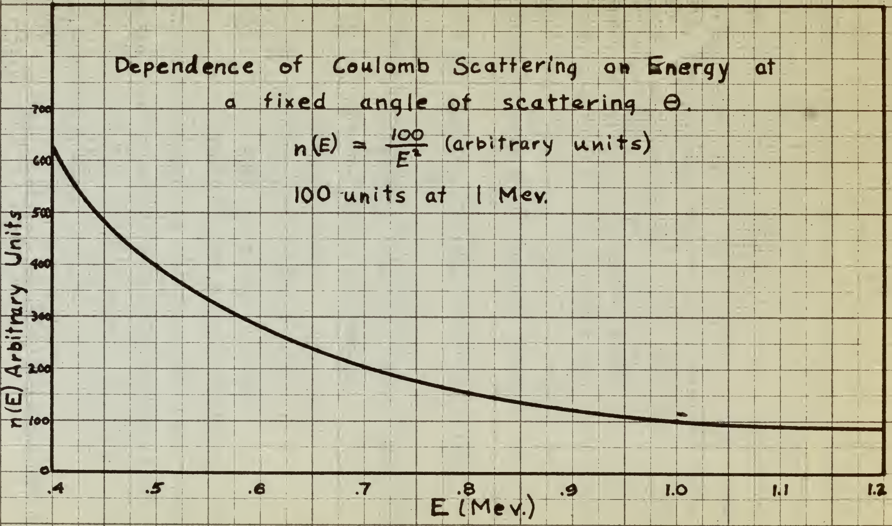
Dependence of Coulomb Scattering on Energy at
a fixed angle of scattering Θ.
$n(E) = \frac{100}{E^2}$ (arbitrary units)
100 units at 1 Mev.
n(E) Arbitrary Units
0
100
200
300
400
500
600
700
.4
.5
.6
.7
.8
.9
1.0
1.1
1.2
E (Mev.)

FIGURE 3.

scattering consist of, it is necessary to look at resonance scattering and nuclear potential scattering. The former occurs when the compound nucleus is formed in an excited state, the latter occurs in that region where the nuclear forces are felt by the incident particle but without the formation of a compound nucleus. For protons on nuclei of much heavier mass, nuclear potential scattering can be considered as small compared to pure Coulomb scattering. For neutrons, however, potential scattering by the nuclear forces is a large factor.

Feshbach, et al.[25] using Breit-Wigner theory, develop a formula for elastic scattering cross-section near a resonance level for particles of angular momentum zero ($l = 0$):

$$\sigma_{sc} = \frac{\lambda}{\pi}^{2} \left| \frac{\Gamma_a}{2(E - E_0) + i\Gamma} + e^{2\pi i a/\lambda} \sin\left(\frac{2\pi a}{\lambda}\right) \right|^{2}$$

where: Γ_a = partial level width due to the reemission of a particle like the incident particle.

Γ = total width of resonance.

a = nuclear radius

E_0 = energy at resonance

E = energy of incident particle

λ = deBroglie wave length of incident particle

The first term between the bars represents the resonance scattering, the second represents the potential scattering. If only potential scattering were present, the scattering cross-section would be given by:

$\sigma_{pot} = \frac{\lambda}{\pi}^{2} \sin^2\left(\frac{2\pi a}{\lambda}\right)$ which is the scattering due to

an impenetrable sphere of radius a.

If potential scattering is neglected, the cross-section becomes that due to a single resonance level:

$$\sigma_{res} = \frac{\lambda^2}{\pi} \cdot \frac{\Gamma_a^{\,2}}{4(E - E_o)^2 + \Gamma^2}$$

Since the magnitude of the potential scattering depends on the term: $\sin\left(\frac{2\pi a}{\lambda}\right)$, it can be assumed that it is negligible at low proton energies due to the increasing value of λ. At proton energies above 0.700 Mev. it does become appreciable; the nuclear radius for A^{40} computed from: $a = 1.5\ A^{1/3} \times 10^{-13}$ cm. is: $a = 5.12 \times 10^{-13}$ cm. and $\lambda = 2.91 \times 10^{-12}$ cm. for a Mev. proton from which the value of $\sin\left(\frac{2\pi a}{\lambda}\right)$ is 0.886 and $\sin^2\left(\frac{2\pi a}{\lambda}\right) = 0.785$.

The combined effects, however, include cross-terms which represent interference phenomena between resonance and potential scattering. At certain phase relations between the two waves, destructive interference occurs and at others, constructive interference occurs.

If there are only two possible outcomes of a nuclear collision, for example, re-emission of the incident particle or formation of a compound nucleus with emission of a different particle, then we speak of partial disintegration constants, Γ_a and Γ_b. These are partial level widths for the two competitive processes and the total level width is simply:

$$\Gamma = \Gamma_a + \Gamma_b .$$

If, however, there are other possible ways for the compound nucleus to break up then the total width is:

$\Gamma = \Gamma_a + \Gamma_b + \sum_x \Gamma_x$, where Γ_x refers to all the other possible modes of disintegration.

For the reaction,

$$a + A \longrightarrow B + b$$

the Breit-Wigner cross-section for emission of particle of type b is given by:

$$\sigma_{AB} = \frac{\lambda^2_a}{\pi} \cdot \frac{\Gamma_a \Gamma_b}{4(E - E_0)^2 + \Gamma^2}$$

This assumes zero angular momentum of the compound nucleus, i.e. $l = 0$, and neglects effects due to spin of particles.

Interference between Resonance Scattering and Coulomb Scattering.

Detection of resonance scattering in the presence of strong Coulomb scattering may be extremely difficult. Devons[19] gives a very simple method for estimating the conditions under which it is possible.

If we assume that no other process than resonance scattering has comparable probability at resonance then we may set $\Gamma = \Gamma_a$ and $E = E_0$. The resonance differential cross-section then reduces to:

$$\sigma_{res} = \frac{\lambda_a^2}{4\pi \cdot \pi} = \frac{\hbar^2}{2\, mE_o}$$

This neglects angular momentum of the compound state and intrinsic angular momenta of the initial nucleus and incident proton. A spin-statistical factor of order unity, g, is introduced by Fermi[26], viz.,

$$g = \frac{1}{2}\left(1 \pm \frac{1}{2 I_A + 1}\right),$$ where I_A = spin of scattering nucleus

$\frac{1}{2}$ = spin of proton

and spin of the compound nucleus, $I_C = I_A \pm \frac{1}{2}$.

Then, the resonance cross-section is:

$$\sigma_{res} \doteq g \cdot \frac{\hbar^2}{2\, mE_o}$$

Representative values of g are:

I_A	0	$+\frac{1}{2}$	$-\frac{1}{2}$	+1	−1
g	1, 0	$\frac{3}{4} \cdot \frac{1}{4}$	(Indet.)	$\frac{2}{3} \cdot \frac{1}{3}$	0, 1

The ratio of resonance scattering to Coulomb scattering at resonance is then:

$$\frac{\sigma_r(\theta)}{\sigma_c(\theta)} = g \cdot \frac{8\, E_o\, \hbar^2}{m(zZe^2)^2} \sin^4\left(\frac{\theta}{2}\right)$$ where m = reduced mass of proton

$$= 3.5 \times 10^5 \cdot \frac{E_o}{Z^2} \sin^4\left(\frac{\theta}{2}\right)$$ E_o = resonance energy in Mev.

assuming g = 1.

In practice, this ratio will be further reduced by a factor, $\frac{\Gamma_r}{\delta E}$ if the level width, Γ_r, is less than the

energy spread, δE, of the scattered protons. Devons[19] points out that resonance scattering will be most readily detectable for small Z, large scattering angles ($\sim 180^\circ$) and for energies E for which the level width (strongly dependent on E due to barrier penetration) is comparable to the experimental resolution and yet not so large that discrete level structure disappears. It is also necessary to assume that there is no other process more probable than elastic scattering.

For proton energy, $E_o = 1$ Mev., scattering angle $\theta = 180^\circ$, using argon as the scattering nucleus, $Z = 18$, the ratio becomes:

$$\frac{\sigma_r}{\sigma_c} = 9.42 \left(\frac{\Gamma_r}{\delta E} \right)$$

In other words, if the energy resolution should be as much as five times the level width, the ratio of maximum resonance scattering to Coulomb scattering (neglecting other processes) would still be about two to one.

Bethe's Formula.

Bethe[27] derived an expression for the ratio of total scattering to Coulomb scattering near a single resonance which includes provision for total angular momentum and spin of the scattering nucleus and incident particle:

$$R = \frac{\sigma}{\sigma_c} = 1 + \frac{2J + 1}{(2i + 1)(2s + 1)} \cdot \frac{\rho^2 + 2\rho \sin \xi + 2\rho x \cos \xi}{(1 + x^2)}$$

where: σ = total scattering cross-section per unit solid angle

σ_c = Coulomb (Rutherford) scattering cross-section

J = total angular quantum number of the compound nucleus

i = spin of scattering nucleus

s = spin of incident particle

$$x = \frac{2\,(E - E_r)}{\Gamma_r}$$

E = energy of incident particle

E_o = energy at resonance

Γ_r = total level width

$$\rho = \frac{2\hbar v}{e^2 zZ}\left[\frac{\Gamma^r_{Pp}}{\Gamma_r}\right]\sin^2\left(\frac{\theta}{2}\right)$$

Γ^r_{Pp} = partial width of resonance level (corresponding to emission of the incident particle P with the scattering nucleus being left in the ground state p)

$$\xi = \alpha \log \sin^2\left(\frac{\theta}{2}\right)$$

θ = scattering angle in center of mass coordinates

$$\alpha = \frac{zZe^2}{\hbar v}$$

v = velocity of incident particle

Z = atomic number of scattering nucleus

z = atomic number of incident particle

$\hbar = \frac{h}{2\pi}$ (Planck's constant)

Rose[28] puts the equation into slightly different form:

$$R = 1 + \frac{\rho_1^2 + 2\,\rho_1 \sin\xi + 2\,\rho_1 x \cos\xi}{1 + x^2}$$

where $\rho_1 = (2J + 1)\left(\frac{2}{\gamma}\right)\left(\frac{\Gamma^r_{Pp}}{\Gamma_r}\right) \sin^2\left(\frac{\theta}{2}\right) P_J(\cos\theta)$

$$\gamma = \frac{zZe^2}{\hbar v}$$

$$\xi = \alpha \log \sin^2\left(\frac{\theta}{2}\right)$$

$P_J(\cos\Theta)$ = Legendre polynomial of order J

$$e^{i\xi} = e^{i\xi_0}\prod_{1}^{J}\frac{(n+i\gamma)^2}{n^2+\gamma^2}$$

If we assume that the only energetically possible process other than scattering of the incident particle is gamma emission and since radiation widths are negligible compared to particle widths, especially for light nuclei, for all practical purposes we may take,

$$\frac{\Gamma^{r}_{Pp}}{\Gamma_r} = 1$$

With this assumption the constants for Bethe's ratio have been computed for the particular experimental arrangement used for the present problem of scattering of protons from argon at an angle of 150°, assuming i = 0 and s = $\frac{1}{2}$ (reference 24).

$$R = \frac{\sigma}{\sigma_0} = 1 + 0.324\ (2J+1)\ (0.260 + 1.962\ x)\ /\ (1 + x^2)$$

If we assume Γ_r = 50 Kev., then x = 40(E - E_0). Using this value and J = 0, the above ratio is plotted in Fig. 4. This curve shows the general shape of an anomaly in the Rutherford scattering. Naturally, this anomaly will be superimposed on the Rutherford scattering curve which is plotted in Fig. 3 for arbitrary units along the ordinate using 100 at an energy of 1 Mev. It will be noted that an increase in J (higher angular momentum quantum number of

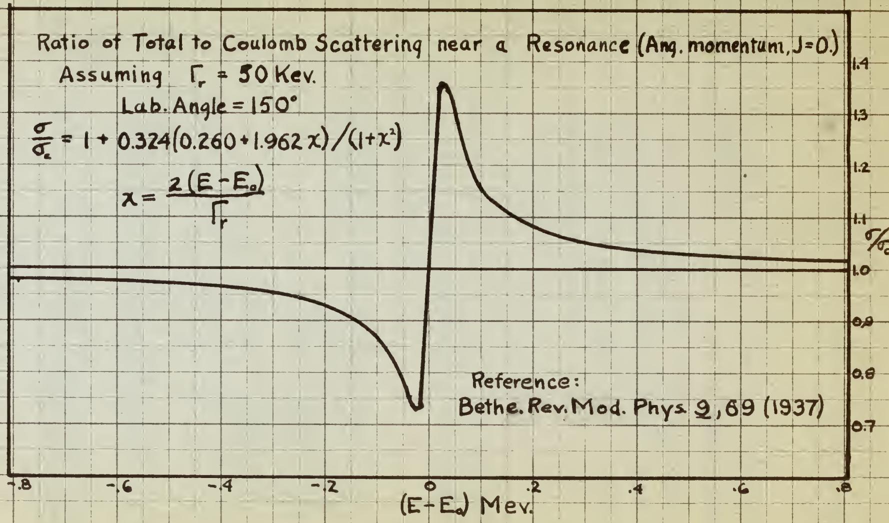
Ratio of Total to Coulomb Scattering near a Resonance (Ang. momentum, J=0.)
Assuming Γ_r = 50 Kev.
Lab. Angle = 150°
$\frac{\sigma}{\sigma_c} = 1 + 0.324(0.260 + 1.962x)/(1+x^2)$
$x = \frac{2(E-E_0)}{\Gamma_r}$
Reference:
Bethe. Rev. Mod. Phys. 9, 69 (1937)
1.4
1.3
1.2
1.1
σ/σ_c
1.0
0.9
0.8
0.7
-.8
-.6
-.4
-.2
0
.2
.4
.6
.8
$(E-E_0)$ Mev.

FIGURE 4.

compound nucleus) serves to increase the magnitude of both the positive peak and the negative peak, but does not change the spread between the peaks. In other words, the anomaly is sharpened.

The plot of $\frac{1}{\sin^4\left(\frac{\theta}{2}\right)}$ in Fig. 2 shows the strong dependence of Rutherford scattering on angle and consequently the advantage of using an angle near 180°. It will be noted that at an angle of 90° the scattering is almost four times that at 150°, whereas at the latter angle it is only 1.15 times the true back scatter at 180°.

Level Widths.

Rose[28] also gives a method for estimating the level width from experimental data. The maximum and minimum scattering ratios are given by:

$$R_{1,2} = 1 + \frac{1}{2}\,\frac{\Gamma_r(E_{1,2})\,b}{E_{1,2} - E_0}$$

where $b = 2\rho\cos\xi$
E_0 = resonance energy
$E_{1,2}$ = energy values at maximum and minimum values of R
$R_{1,2}$ = maximum and minimum values of R

Since the only unknown is Γ_r, the level width can be found from this formula.

Also the level width without Coulomb barrier may be found from:

$$\Gamma_r = G_r\,P$$

where G_r = level width without Coulomb barrier

P is the penetrability calculated from well known formulae by Bethe[27]. Rose also gives a simple method of determining J if interference scattering is neglected at the extrema of the anomaly. The extrema are also given by:

$$R_{1,2} = 1 + \frac{b}{2x_{1,2}} \quad \text{and} \quad x_{1,2} = -\frac{a}{b} \mp \left(1 + \frac{a^2}{b^2}\right)^{\frac{1}{2}}$$

combining,

where $a = \rho^2 + 2\rho \sin\zeta$
$b = 2\rho \cos\zeta$

$$\rho = \pm\left(R_1^{1/2} - R_2^{1/2}\right)$$

and since ρ is also given by definition to be:

$$\rho = (2J+1)\left(\frac{2}{\gamma}\right)\left(\frac{\Gamma^r_{pn}}{\Gamma_r}\right)\sin^2\left(\frac{\theta}{2}\right)P_J(\cos\theta)$$

$$\text{where } \gamma = \frac{Zze^2}{\hbar v}$$

the only unknown parameter is J.

Resonance energy always lies between the extrema. The maximum error therefore in taking it to lie midway between would be one-half the separation between extrema or about one-fourth of the level width. The effect of straggling, i.e., beam spread in energy through the target, in shifting the higher extremum toward higher energies and lower energy extremum toward lower energies, thus increasing their separation by about the straggling width, increases the uncertainty in the resonance energy by a like amount.

Recent Experiments.

Two groups at the University of Wisconsin have recently demonstrated the power of using elastic scattering to investigate excited levels in light nuclei.

Bender, Shoemaker, Kaufmann, and Bouricius[29] have investigated the 985. Kev. resonance in Al^{27} by means of the elastic scattering of protons. The variation in scattering yield is in very good agreement with the above theory near the resonance. Elastic scattering of protons from Mg^{24} was investigated throughout a range of proton energy from 0.40 to 3.95 Mev. by Mooring, Koester, Goldberg, Saxon, and Kaufmann.[30] Anomalies of varying shapes other than the type shown in Fig. 4 were discovered. The general discussion of the theory of such anomalies has been made by Laubenstein and Laubenstein[31]. This theory includes not only the interference caused by phase shifts induced by energy levels of the compound nucleus but also that due to the hard sphere type of scattering. A vector method of analysis of anomalies is given which enables one to calculate the shape of anomalies based on an assumption of the total angular momentum of the compound nucleus. The predicted shapes for the various arbitrary values of J chosen can be compared with the curves from experimental data. The "best fit" then can be assumed to yield the correct value of J.

In a later article Koester[32] gives a fairly complete

analysis of the resonances found in Mg^{24} by Mooring, Koester, et al. along the line of the theory just mentioned. He points out that the parity P of the excited nucleus is related to the parity p of the ground state of the target nucleus by the expression,

$$P = (-1)^L p$$

where L is the orbital angular momentum value of the incident proton with spin value $\frac{1}{2}$. The value of L is given by,

$$J = L \pm \frac{1}{2}$$

for target nuclei of spin zero. Since the qualitative shape of a resonance anomaly depends strongly on particular values of J and L, the angular momentum and parity number of energy levels can be determined.

Since A^{40} is a nucleus of zero spin, it satisfies the requirements of the above theory.

We have seen that the following information can be obtained from an analysis of anomalies in elastic scattering of protons on nuclei of spin zero:

(a) Energy levels of excited states of the compound nucleus,

(b) Angular momentum of excited states of the compound nucleus,

(c) Relative parity numbers of the excited states,

(d) Level widths of the resonances, and

(e) Level widths without Coulomb barrier.

IV. APPARATUS: DESCRIPTION, CALIBRATION, BASIC CALCULATIONS

Mechanical Parts.

The apparatus originally designed by Commander A. B. Chilton[33], U.S. Navy, during his graduate work at The Ohio State University is shown in Fig. 6. It consists of five principal parts: (1) a connecting piece which attaches to the end of the proton tube in the magnetic analyzing section of the Van de Graaff generator; (2) the beam collimator which restricts the proton beam to a diameter of 0.1" and directs it into the reaction chamber; (3) the reaction chamber which serves also as a Faraday cage, in which the proton reaction occurs and the ion current is collected after passing through a nickel foil window; (4) the reaction collimator consisting of three collinear ports, 0.06" in diameter, alligned at a laboratory angle of 150° from the proton beam, and which serves to define the target area and to align the scattered particles entering the detection chamber; and (5) the counter itself, which is a typical gas-filled proportional counter collecting ionization pulses from the collimated beam of reaction or scattered particles entering via the reaction collimator. The last of the three small 0.06" ports in the reaction collimator is mechanically integral with the proportional counter, being in the end wall of the sensitive chamber.

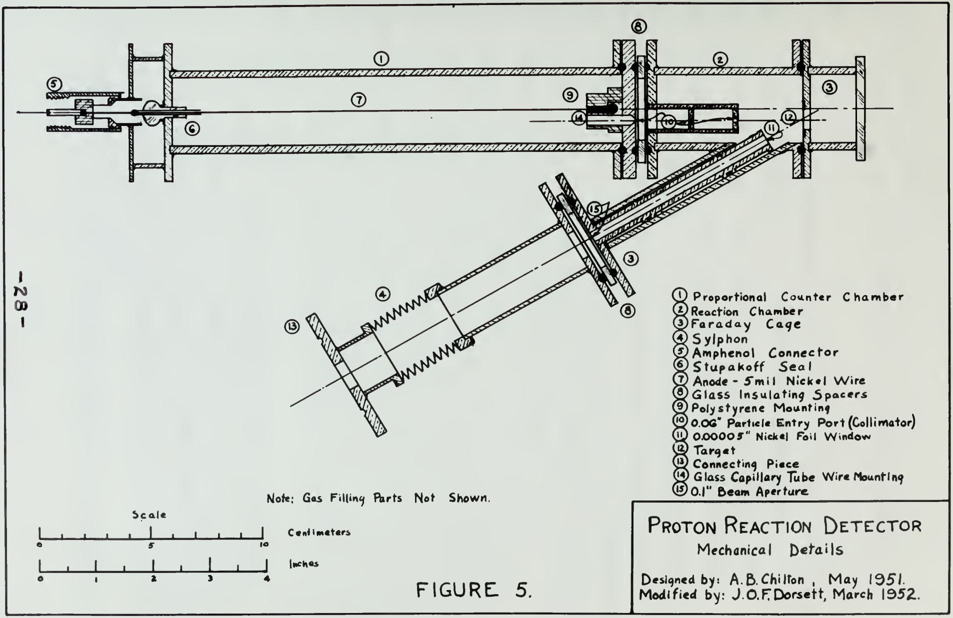
①
②
③
④
⑤
⑥
⑦
⑧
⑨
⑩
⑪
⑫
⑬
⑭
⑮
① Proportional Counter Chamber
② Reaction Chamber
③ Faraday Cage
④ Sylphon
⑤ Amphenol Connector
⑥ Stupakoff Seal
⑦ Anode - 5mil Nickel Wire
⑧ Glass Insulating Spacers
⑨ Polystyrene Mounting
⑩ 0.06" Particle Entry Port (Collimator)
⑪ 0.00005" Nickel Foil Window
⑫ Target
⑬ Connecting Piece
⑭ Glass Capillary Tube Wire Mounting
⑮ 0.1" Beam Aperture
Note: Gas Filling Parts Not Shown.
Scale
0
5
10
Centimeters
0
1
2
3
4
Inches
PROTON REACTION DETECTOR
Mechanical Details
Designed by: A.B. Chilton, May 1951.
Modified by: J.O.F. Dorsett, March 1952.

FIGURE 5.

This end wall of the counter also serves as an electrostatic shield between the Faraday cage and sensitive volume.

Certain modifications have been made in the original design. These include: (1) glass insulating rings substituted for lucite; (2) except for the entry port, completely enclosing the sensitive volume with brass to avoid spurious counts due to a capacity which formerly existed between the floating end of the central wire and the Faraday cage; (3) addition of the reaction collimator and modification of the proton beam collimator; (4) changing all internal valves to the bellows type needle valve.

The reaction collimator serves to limit the extent of the proton beam from which the scattered protons are being counted. The geometry of the apparatus is such that the extreme thickness of the gaseous target under surveillance is about 1.3 centimeter. Since the argon is under a reduced pressure of 75 mm. Hg, the equivalent thickness at standard pressure is about 1 mm.

The counting chamber is operated in the proportional region. It is fitted with a gas manifold providing connections to gas tanks, vacuum pump, and mercury manometer. Multiple connections allow mixtures to be used and permit flexibility of pressure control.

A nickel foil window, 0.05 mil thick at the end of the

beam collimator provides a vacuum seal between the reaction chamber and the Van de Graaff vacuum system. This foil is designed to withstand a pressure of one atmosphere against the outer side; but in actual operation no more than 250 mm. Hg is ever necessary since a vacuum cross connection permits simultaneous evacuation of all parts of the apparatus. After the vacuum is obtained, the valve in the cross connection can be closed thus isolating the manifold and counting chamber from the Van de Graaff vacuum system.

The central wire of the proportional counter is a 5 mil nickel wire supported at the free end in a glass capillary bulb enclosed in a polystyrene mounting. The other end passes through a Stupakoff seal and thence to an amphenol connector which attaches directly to the preamplifier.

Electronic Apparatus

The preamplifier is an Atomic Instrument Co. Preamplifier 205-B, originally built to be used with an ionization chamber with a time constant of 2.7 milliseconds. The time constant has been changed to 7.5 microseconds to make it appropriate for use with a proportional counter at fast counting rates. This instrument has two stages of amplification and two cathode followers incorporating inverse feedback to achieve a high order of gain stability. Pulse amplification is fixed at approximately 20. A special high voltage coaxial cable was built to allow voltages up to 1200 volts to be impressed on the central wire of the proportional

counter. Filament and plate voltages are supplied by a Model 204-B amplifier built by Atomic Instrument Co.

The output from the pre-amplifier is fed to the Model 204-B Linear Amplifier. The gain from this instrument is not too essential when used with the 205-B Pre-amplifier; the amplifier is used as a pulse shaper and discriminator. A pulse amplitude discriminator passes all pulses received above that voltage set on the discriminator dial. Linearity of dial setting is better than 2% from 0 to 100 volts. Three different rise times are provided: 5, 0.8, and 0.2 microseconds with decay times of about 25, 4, and 0.4 microseconds. Output from the discriminator is a constant 10 volt, 0.4 microsecond pulse which is fed to a Model 1030 Atomic Instrument Co. Scaler. An oscilloscope is operated from the high level output of the amplifier.

High voltage power for the central wire of the proportional counter is obtained from a Model 1090, 5000 volt Regulated Power Supply built by Nuclear Instrument and Chemical Corporation. This power source can supply either positive or negative voltage from zero to maximum value with regulation to within 0.02% of output voltage.

A sensitive integrator is connected to the Faraday cage to determine the total proton ion charge collected. This instrument was designed and built by W. E. L. Boyce[34] during his graduate work at The Ohio State University in 1951-1952.

The integration is accomplished by collection of positive charge on a special polystyrene condenser having a capacity of 0.982 microfarad, which is charged to a negative potential of about 10 volts, the exact value must be measured at the charging battery. The integrator has a controlling relay which operates the scaler so that it registers only during the integration period. The instrument may be set to operate for several different specified cycles of charge and discharge of the integrating condenser from one cycle to 24 cycles of operation, depending on the intensity of the proton beam. One cycle of the integrator will be equivalent to a charge given by the following expression:

$$Q = CV = 0.982V \quad \text{where } V = \text{battery voltage}$$
in microcoulombs

If the battery is exactly 10 volts, the charge will be 9.82 microcoulombs which is equivalent to 6.13×10^{13} protons. The design was such that one cycle would be approximately equivalent to collection of 10 microcoulombs or 6.24×10^{13} protons. A counting period of ten seconds would therefore mean a beam current of 1 microampere. The error of the integrator for ion currents greater than 0.06 microampere due to leakage is less than ± 1%. For charging voltages of about 10 volts the error in collected charge due to leakage is therefore less than ± 0.1%. For runs of length greater than 10 seconds (i.e. currents less than 1 microampere) the error due to relay time is less than 0.5%.

The integrator appears to be dependable to within ± 1% for ion beam currents of 0.06 to 1 microampere.

The electronic and gas filling systems are shown in Fig. 6. A positive potential of +90 volts is maintained on the insulated connecting piece to prevent secondary electrons scattered from the first port of the beam collimator from being collected in the Faraday cage and thus giving an erroneous integration of beam current.

Calibration.

The proton energy resolution is determined by a 1 mm. slit 70 cm. from the center of the magnet pole faces. The beam at this point has been deflected through an angle of 30° from the neutral beam axis of the Van de Graaff. The resolution is calculated as follows:

Let L = length of magnet pole face.
r = radius of arc along which the beam is deflected between magnet pole faces.
A = angle through which beam is deflected.

Then,

$$L = r \sin A$$

$$\frac{dr}{r} = -\cot A \, dA$$

$$dA = 0.1 \text{ cm}/\ 70 \text{ cm.} = 1.43 \times 10^{-3}$$

Therefore,

$$dr/r = -2.48 \times 10^{-3}$$

Neglecting the variation of the magnet current, dr/r is approximately equal to $dE/2E$ since r is proportional to $\sqrt{E}$. Using this approximation,

$$dE/E = 0.5\%$$

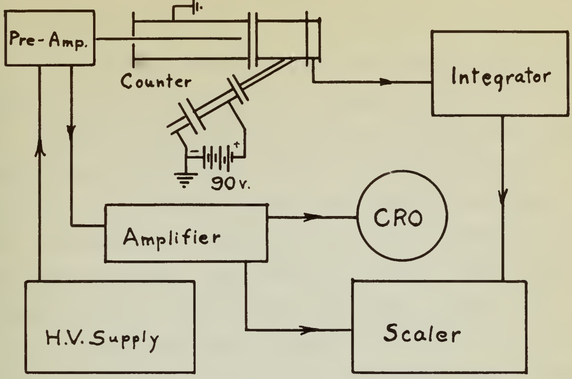

ELECTRICAL CONNECTIONS

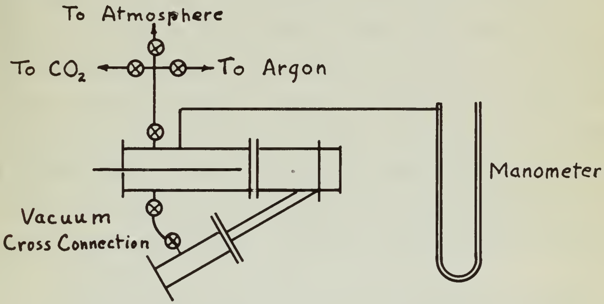

GAS AND VACUUM CONNECTIONS

FIGURE 6.

or at an energy of 1 Mev., $dE = 5$ kev.

The magnet was calibrated for this slit setting on the 0.873 Mev. gamma resonance of F^{19} using a LiF target.

Amplification factors for the gas amplification in the proportional counter were obtained by using an internal source of alphas consisting of a thin layer of polonium salt evaporated on a tantalum disc. This was inserted in the target mounting. The counter was filled with various pressures and at each one the central wire voltage was varied. Pulse sizes were determined by observation on an oscilloscope. In actual practice, the pulse size was maintained constant on the screen of the oscilloscope by varying the gain on the linear amplifier. The reference point was taken as that gain necessary to produce the pulse height with the counter voltage so low that amplification was essentially unity, i.e., when the counter was operating in the ionization chamber region. Reciprocals of gain settings for a given constant pressure then became the relative amplification factors of the counter tube assuming the gain setting for the ionization region represented an amplification of unity. Curves of amplification factors are plotted in Figure 7.

A discriminator curve was run on the internal Po^{210} source. Data are given in Table I, and the curve is plotted in Figure 8.

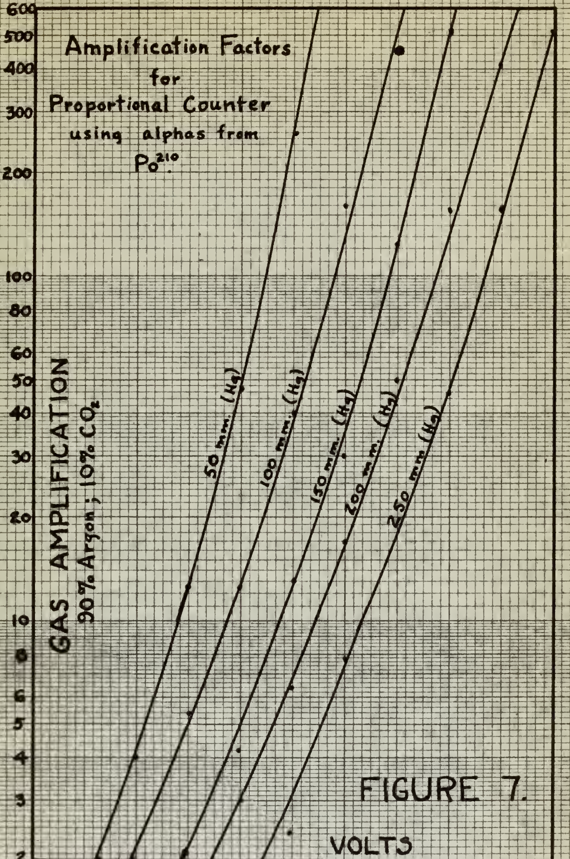

Amplification Factors for Proportional Counter using alphas from Po^{210}.

FIGURE 7.

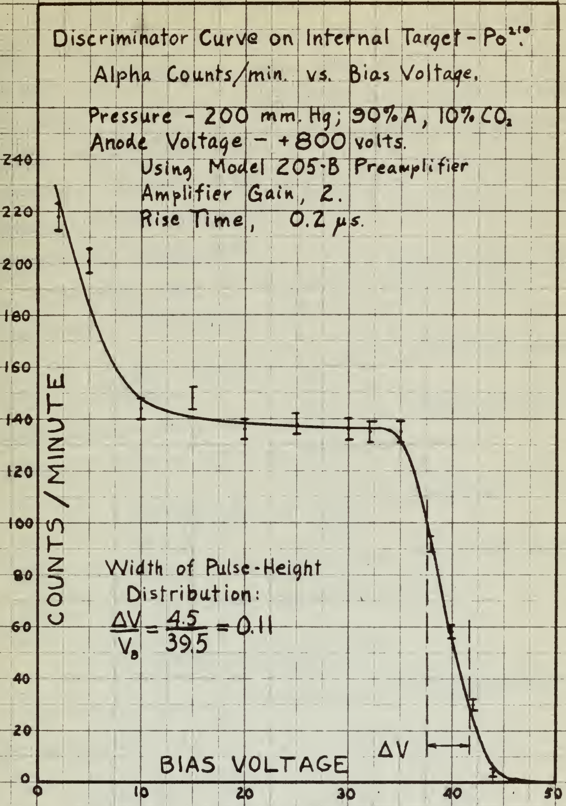
Discriminator Curve on Internal Target - Po^{210}.
Alpha Counts/min. vs. Bias Voltage.
Pressure - 200 mm. Hg; 90% A, 10% CO_2
Anode Voltage - +800 volts.
Using Model 205-B Preamplifier
Amplifier Gain, 2.
Rise Time, 0.2 μs.
Width of Pulse-Height Distribution:
$\frac{\Delta V}{V_B} = \frac{4.5}{39.5} = 0.11$
ΔV
COUNTS / MINUTE
BIAS VOLTAGE
240
220
200
180
160
140
120
100
80
60
40
20
0
0
10
20
30
40
50

FIGURE 8.

Since the target for scattering from argon is a gaseous target, it was necessary to resort to actual measurements of the geometry of the reaction volume to determine the target thickness from which the energy spread in the target was computed. Similarly, the distances from target volume to sensitive volume of the counter were measured. These distances are recorded in Table II along with other experimental measurements.

The solid angle at the reaction subtended by the 0.06" entry port at the counter wall was computed to be:

$d\Omega_0 = \frac{1}{3144}$ steradian for the mean distance of 7.55 cm. from target to entry port. Since the entry port has a diameter of 0.06" or 0.152 cm. the computation is:

$$d\Omega_0 = \frac{(0.152)^2\,\pi}{4 \times (7.55)^2} = \frac{1}{3144} \text{ steradian.}$$

From the geometry of the reaction collimator the parallax subtended by the target is computed to be:

$$d\theta_1 = \frac{0.152}{2.3} = 0.0663 \text{ radian}$$

The variation in scattering angle (laboratory system) is therefore,

$$\frac{d\theta_1}{2} = d\theta_0 = \pm 1.9^\circ$$

The laboratory scattering angle is then,

$$\theta = 150^\circ \pm 1.9^\circ.$$

Basic Calculations.

The conversion of scattering angle from the laboratory system to the center of mass system is accomplished by the relation,

$$\theta_{cm} = \theta + \arcsin\left[\frac{M_p}{M_A}\sin\theta\right]$$

where θ_{cm} = scattering angle, center of mass
θ = scattering angle, laboratory
M_p = mass of proton
M_A = mass of scattering nucleus

Substituting values for mass of argon nucleus and laboratory angle,

$$\theta_{cm} = 2.6180 + \arcsin\left[\frac{1}{40} \times 0.5\right] = 2.6180 + 0.0125 \text{ (radians)}$$

$$\theta_{cm} = 2.6305 \text{ (radians)}$$
$$\cong 151^\circ 43.1'$$

The reduced mass of the proton for elastic collision with an argon nucleus is:

$$M = \frac{M_p M_A}{M_p + M_A} = \frac{40.08}{40.95} = 0.983 \text{ amu}$$
$$= 1.642 \times 10^{-24} \text{ gram.}$$

Energy conversion from the laboratory system to the center-of-mass system is given by:

$$E = E_o \left[\frac{M_A}{M_A + M_p} \right] = \frac{39.94}{40.95} E_o$$

$$E = 0.975 E_o$$

In order to determine what the energy of the proton is at the scattering nucleus, it is necessary to calculate the loss in energy of the beam while passing through the nickel window and the filling gas between the window and reaction volume.

Chilton[35] has computed the energy thickness of the 0.00005" nickel foil window for various energies of protons. The energy of the beam minus this value is the net energy available in the reaction chamber at the window. This has been plotted as Curve I in Figure 10.

In computing the loss in energy due to passage through the filling gas, we make use of the range tables for pure argon based on experimental and theoretical considerations by Hirschfelder and Magee[35]. These data are plotted as a range curve in Figure 9. The presence of 10% CO_2 is not considered to effect the correctness of the calculations owing to the uncertainities of the basic data and the inaccuracies of measurement of the dimensions of the apparatus.

Furthermore, the presence of 10% CO_2 is not considered

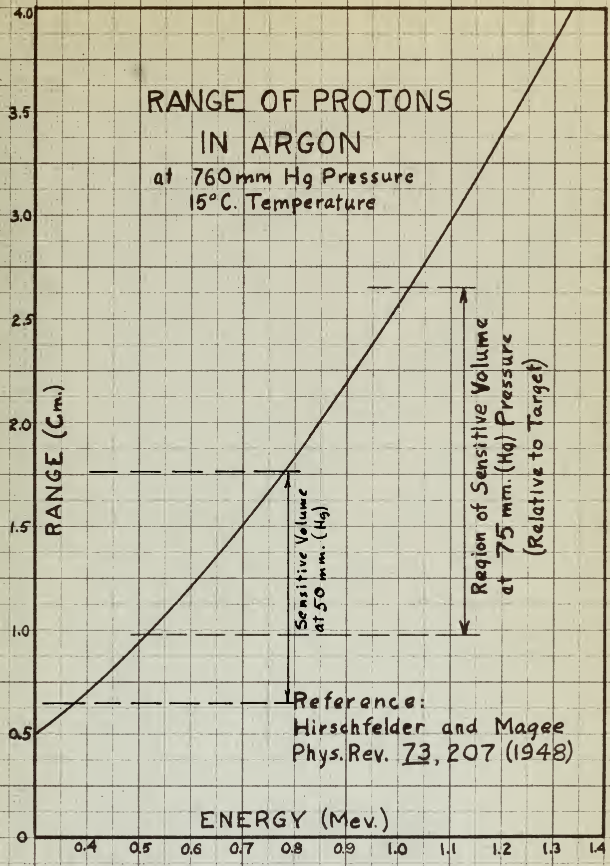
RANGE OF PROTONS
IN ARGON
at 760mm Hg Pressure
15°C. Temperature
RANGE (Cm.)
ENERGY (Mev.)
4.0
3.5
3.0
2.5
2.0
1.5
1.0
0.5
0
0.4
0.5
0.6
0.7
0.8
0.9
1.0
1.1
1.2
1.3
1.4
Sensitive Volume at 50 mm. (Hg)
Region of Sensitive Volume at 75 mm. (Hg) Pressure (Relative to Target)
Reference:
Hirschfelder and Magee
Phys. Rev. 73, 207 (1948)

FIGURE 9.

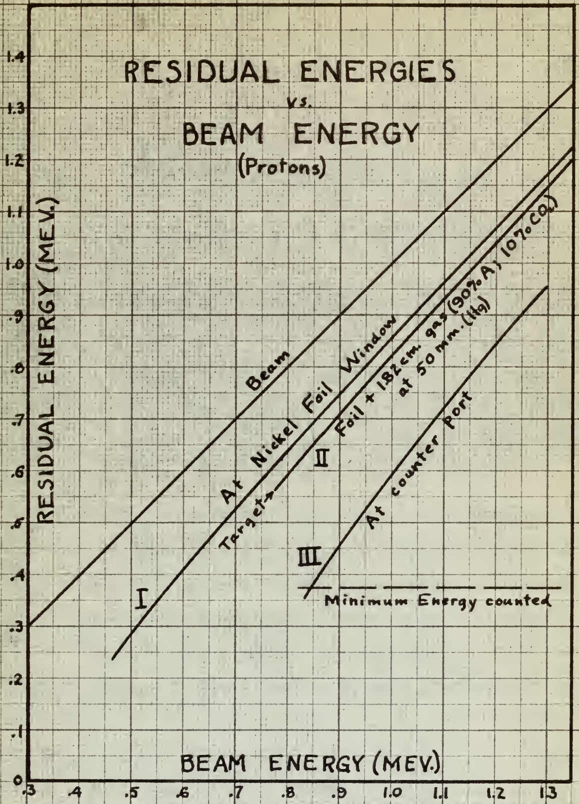
RESIDUAL ENERGIES
vs.
BEAM ENERGY
(Protons)
RESIDUAL ENERGY (MEV.)
BEAM ENERGY (MEV.)
0
.1
.2
.3
.4
.5
.6
.7
.8
.9
1.0
1.1
1.2
1.3
1.4
.3
.4
.5
.6
.7
.8
.9
1.0
1.1
1.2
1.3
Beam
At Nickel Foil Window
I
Target→
Foil + 182 cm. gas (90% A; 10% CO2)
at 50 mm. (Hg)
II
At counter Port
III
Minimum Energy counted

FIGURE 10.

to have any appreciable effect on the intensity of Coulomb scattering inasmuch as the cross-section for this type of scattering is proportional to the fourth power of Z. The average Z for CO_2 is 7.3 while for A it is 18. The ratio of cross-section due to argon to that due to CO_2 (based on 90% A, 10% CO_2) is:

$$\frac{\sigma_A}{\sigma_{CO_2}} = \frac{18^4 \times 0.9}{7.3^4 \times 0.1} = \frac{9.45 \times 10^4}{187} = 500$$

In other words the maximum error in neglecting the 10% CO_2 is about 0.2%.

We may proceed to a calculation of the energy losses in the various portions of the reaction and counting chambers using the experimental measurements and the range curve for argon. The filling gas is at a pressure of 75 mm. Hg so all range measurements must be reduced by the factor, 75/760.

Table III is a computation of residual ranges and corresponding energies in argon at the extremities of the reaction volume for various initial beam energies. The difference between these energies is the spread in energy of elastically scattered protons due to thickness of the gaseous target. It is one factor in the experimental resolution.

Table IV is a computation of residual ranges and corresponding energies of elastically scattered protons upon reaching the sensitive volume of the counter. The spread

in these energies is a measure of the difference in pulse sizes produced by the proportional counter. It will be noted that a large spread in these energies will give an apparent increase in counting rate as energy is increased above the threshold energy for counting, contrary to the theoretical reciprocal relation of Coulomb scattering to energy squared (Figure 3.) That is, the counting rate will increase until the entire spread of elastically scattered protons are entering the proportional counter. This occurs when the scattered proton has an energy (laboratory system) of about 535 kev. This value is arrived at by taking the distance from target to counter (see Fig. 9) which is the range of the minimum energy which can just reach the counter or 515 kev. and adding the straggling of 20 kev.

__Sample Computation for Table III.__

Beam energy	1 Mev.	Range	2.56 cm.
Loss in Ni window	-0.145 Mev.		
E at internal face of Ni	0.855	Range	2.03 cm.

Distance to reaction volume:

Minimum	1.30 cm.	Equivalent	Range	0.128cm.
Maximum	2.35	"	"	0.230

Residual ranges of elastically protons:

Maximum, 2.03 - 0.128 = 1.90 cm.	Energy,	0.820 Mev.
Minimum, 2.03 - 0.230 = 1.80 cm.	"	0.792 "

Energy thickness of target,	0.028 Mev.
Average energy of elastically scattered protons,	0.806 "

Sample Computation for Table IV.

Reaction ranges and energies:	R	E
Maximum	1.90 cm.	0.820 Mev.
Minimum	1.80 cm.	0.792 "

Distances to sensitive volume:		Equivalent ranges:
Maximum	10.4 cm.	1.028 cm.
Minimum	9.4 cm.	0.929 cm.

Residual ranges and energies in counter:	R	E
Maximum (1.90 - 0.929)	0.97 cm.	0.513 Mev.
Minimum (1.80 - 1.028	0.77 cm.	0.427 "

Spread in range,	0.20 cm.	
Spread in energy,		0.086 Mev.
Average energy of counted protons,		0.470 "

Spread in actual distance travelled in counter, 2.13 cm. This is the worst possible condition and not the most probable. To arrive at the most probable spread in energies and therefore pulse sizes and energy resolution, we may treat the subject completely as a straggling problem.

Straggling.

No account has so far been taken of straggling in the nickel foil or in the filling gas, or of beam resolution due to slit width.

Straggling in the nickel foil and argon gas has been treated as far as present theory permits by Chilton[33] who has computed the straggling for the particular case from a formula credited to Madsen and Venkateswarlu[36].

$$\Omega^2 = \frac{4\ z^2 e^4}{M} \cdot \frac{Z_0 t}{A}$$

where,

Ω = standard deviation in energy loss (ergs)
M = weight of particle (g.)
t = thickness of stopping medium (g/cm^2)

Substituting data for Ni foil of thickness 0.00005" (equivalent to 1.13 mg/cm^2) yields:

$$\Omega^2_{Ni} = 2.11 \times 10^{-16} \text{ ergs}^2$$

$$= 0.825 \times 10^{-4} \text{ Mev.}^2$$

$$\Omega_{Ni} = 0.0091 \text{ Mev.}$$

For the gas from window to reaction volume the average distance is 1.82 cm. At atmospheric pressure one centimeter of the gas is equivalent to 1.78×10^{-3} g/cm^2. For 1.82 cm. of gas at 75 mm. pressure we find the thickness to be:

$$1.82 \times 1.78 \times 10^{-3} \times \frac{75}{760} = 3.20 \times 10^{-4} \text{ g/cm.}$$

Substituting this into the formula we get for the gas:

$$\Omega^2_{A} = 0.143 \times 10^{-16} \text{ ergs}^2$$

$$= 0.0559 \times 10^{-4} \text{ Mev}^2$$

$$\Omega_{A} = 0.00236 \text{ Mev.}$$

We may assume from the geometry of the reaction volume that more than 50% of the reaction takes place in a geometrical 50% zone straddling the mid-point of the target. Therefore, if the extreme energy spread in the target is 28 kev. (for aninitial beam energy of 1 Mev.) we

can assume that more than 50% of the elastically scattered protons will have an energy spread of less than 14 kev. If we consider this as a form of straggling we may combine this figure with the straggling due to the Ni window and that due to gas between window and target, and with the beam resolution of 5 kev. defined by the 1 mm. slit.

$$\Omega \cong \left[\Omega^2_{slit} + \Omega^2_{Ni} + \Omega^2_{A} + \Omega^2_{targ}\right]^{1/2}$$

$$\cong \left[(25 - 82.5 - 5.6 - 196) \times 10^{-4}\right]^{1/2} \text{ Mev.}$$

$$\cong 0.0176 \text{ Mev.}$$

This is a conservative value for the most probable experimental resolution attained in the elastic scattering reaction. If the mean energy at the target is 0.806 Mev., the experimental resolution is therefore 2.2%.

Curve II of Figure 10 is the mean energy of the reaction vs. the beam energy.

Curve III of Figure 10 is the mean energy of elastically scattered protons reaching the sensitive volume of the counter. The sensitive volume relative to target is indicated on the range curve of Figure 9. This shows that an elastically scattered proton with an energy of 0.515 Mev. will just reach the sensitive volume at a pressure of 75 mm. Hg and that a scattered proton of 1.020 Mev. energy will reach the extreme limit of the sensitive volume. Since

the Bragg ionization curve shows that the major portion of ionization of a charged particle travelling through a gas is near the end of its track, the particles with an initial reaction energy of 0.9 to 1.0 Mev. will be most efficiently counted at a pressure of 75 mm. Hg. This is the condition desired for investigating a resonance level near 0.900 Mev.

V. EXPERIMENTAL RESULTS

Some of the experimental difficulties encountered were: (1) use of a nickel window required beam energies considerably in excess of energies desired in the reaction, (2) requirements of a moderate counting rate necessitated a small restricting aperture which cut down ion current approximately to 0.1 to 0.5 microcoulombs, (3) a 1 mm. slit for modest beam resolution combined with the restricting beam aperture required some finesse in aligning apparatus, and (4) gas pressure in the reaction and counting chambers had to be reduced to 50 mm. (Hg) pressure in order to raise the minimum energy of scattered protons reaching the sensitive volume. The extent of the sensitive volume at 50 mm. (Hg) has been added to the range-energy curve in Figure 9 in addition to the delineation of this region for 75 mm. (Hg) pressure. With this pressure the minimum energy scattered protons, which reach the sensitive volume, is 375 kev., and the energy of protons which just reach the far end of the sensitive volume is 780 kev. This means that protons which are scattered with an energy of greater than 780 kev. will produce slightly less ionization than those just below the 780 kev. level. This was found to be true in actual operation; and consequently, amplifier gain had to

be set up to about 14 in order that pulses would be large enough to insure counting all protons with a fixed bias voltage.

Two runs were made counting the scattered protons from argon gas at 50 mm. (Hg) pressure. Run #1 was made over the range of incident proton energies from 690 kev. to 1100 kev. inclusive. The data for this run are plotted in Figure 11. This curve shows a definite anomaly at 908 Kev. An arbitrary Coulomb scattering curve is superimposed showing a definite rising trend away from pure Coulomb scattering. This can be attributed largely to a nuclear scattering of the hard sphere type.

The Coulomb cross-section per unit solid angle is:

$$\sigma_c = \left[\frac{zZe^2}{4E}\right]^2 \cdot \frac{1}{\sin^4\left(\frac{\theta}{2}\right)}$$

where $E = \frac{1}{2}\mu v^2$ (ergs)

$\mu =$ reduced mass of proton

$= 1.63 \times 10^{-24}$ g.

The cross-section per unit solid angle due to a hard sphere type of scattering is:

$$\sigma_p = \frac{\lambda^2}{\pi} \sin^2\left(\frac{2\pi a}{\lambda}\right)$$

where $\lambda = \frac{h}{\mu v}$

$a =$ interacting distances between nuclei

$= 1.5\ A^{1/3} \times 10^{-13}$ cm.

$= 5.12 \times 10^{-13}$ cm.

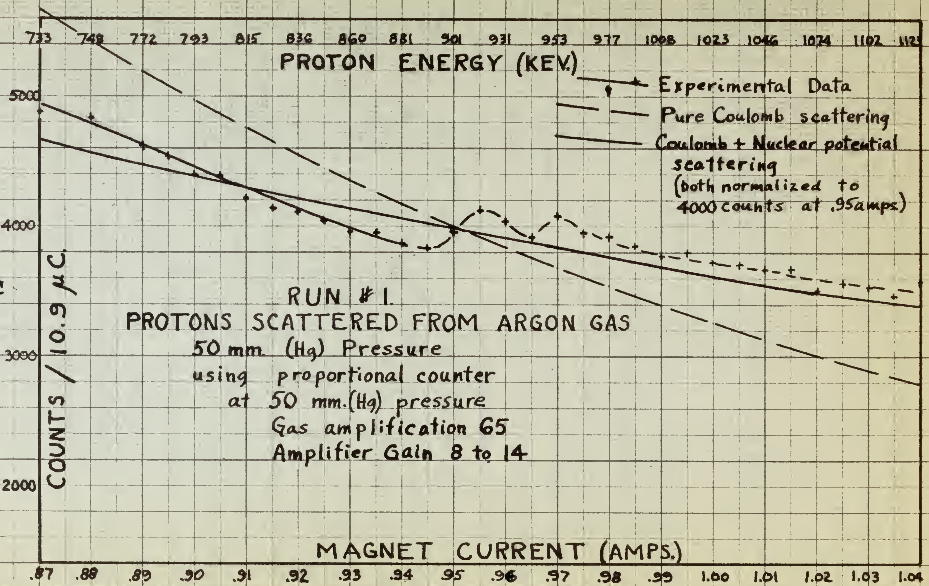
PROTON ENERGY (KEV.)
733
748
772
793
815
836
860
881
901
931
953
977
1008
1023
1046
1074
1102
1125
Experimental Data
Pure Coulomb scattering
Coulomb + Nuclear potential scattering
(both normalized to 4000 counts at .95amps.)
COUNTS / 10.9 μC.
5000
4000
3000
2000
RUN #1.
PROTONS SCATTERED FROM ARGON GAS
50 mm (Hg) Pressure
using proportional counter
at 50 mm.(Hg) pressure
Gas amplification 65
Amplifier Gain 8 to 14
MAGNET CURRENT (AMPS.)
.87
.88
.89
.90
.91
.92
.93
.94
.95
.96
.97
.98
.99
1.00
1.01
1.02
1.03
1.04

FIGURE 11.

If we neglect interference between Coulomb and nuclear potential scattering and attribute the total cross-section to a sum of the two effects,

$$\sigma = \sigma_c + \sigma_p$$

Now, the number of collected scattered particles counted in a solid angle of 1/3144 steradian is:

$$n(\theta) = n_0 N t \sigma / 3144$$

where n_0 = number of incident particles
N = number of atoms / cc.
t = thickness of target (cm.)

t is the only parameter not known with any degree of accuracy, but the shape of the scattering section of the gaseous target is that of a narrow cone intersecting a narrow cylinder at an angle of 30°. The extreme thickness of target section is 1.03 cm., but the effective thickness is somewhere between 0.20 and 0.50 cm. If we assume this effective thickness to be 0.366 cm. the number of collected scattered particles at an energy of 900 kev. is 4000 per 10.9 microcoulombs. These conditions then represent the existing conditions at the cross-over of the anomaly.

Using this value of t = 0.366 cm. and other experimental conditions, the values of σ and $n(\theta)$ were computed and tabulated in Table V. These assumptions are not considered to be out of line from most probably circumstances, and it will be noted that a plot of $n(\theta)$ for various ener-

gies falls very close to the experimental curve obtained except for the anomaly.

From a calibration run on a LiF target the proton energy at the cross-over of the anomaly is 908 kev. Experimental resolution of only about 20 kev. prevents an accurate location of the maximum and minimum points of the anomaly.

This result agrees well with the resonance level of 900 kev. found in argon by Brostrøm, Huus, and Koch[21] in 1948. It demonstrates also that anomalies in elastic scattering of protons may be detected by this method of using a proportional counter even for atoms with Z-number up to 18.

A second run was made which verifies not only the existence of the anomaly at 908 kev. but a smaller anomaly reappears and is suggested as being superimposed on the principal one at an energy of about 945 kev. There was apparently a shift in magnet calibration between the first run and the second; but the energy spread in the anomaly and the energy difference between the two anomalies is the same. The first calibration on the LiF target is assumed correct. The second run is shown in Figure 12. A very slight variation in counting rate is noted but this may be due to inaccuracy in adjusting the gas pressure in the chamber.

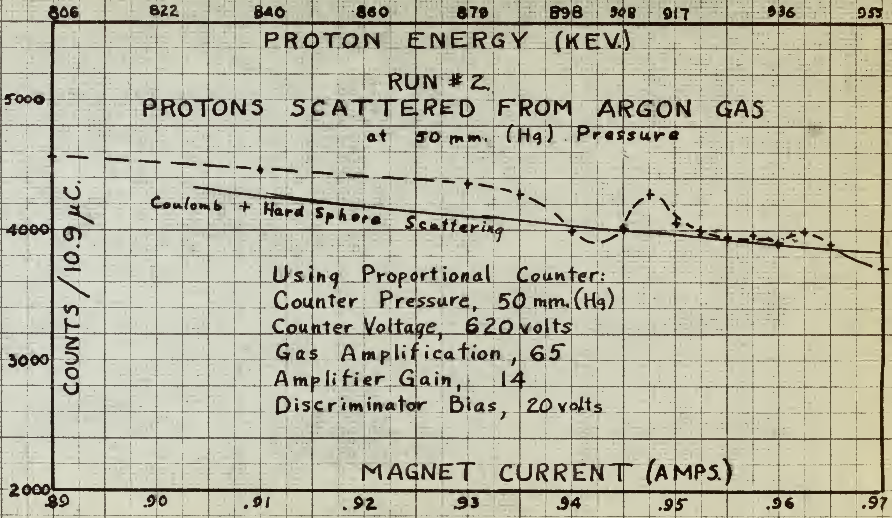
806
822
840
860
878
898
908
917
936
955
PROTON ENERGY (KEV.)
RUN #2.
PROTONS SCATTERED FROM ARGON GAS
at 50 mm. (Hg) Pressure
5000
4000
3000
2000
COUNTS / 10.9 μC.
Coulomb + Hard Sphere Scattering
Using Proportional Counter:
Counter Pressure, 50 mm. (Hg)
Counter Voltage, 620 volts
Gas Amplification, 65
Amplifier Gain, 14
Discriminator Bias, 20 volts
MAGNET CURRENT (AMPS.)
.89
.90
.91
.92
.93
.94
.95
.96
.97

FIGURE 12.

The magnet calibration is indicated on Figures 11 and 12 with the anomaly located at 908 kev. in Figure 12.

A discriminator curve on scattered protons at energy of 650 kev. at the port of the proportional counter is shown in Figure 13.

Conclusions.

(1) A resonance level in K^{41} has been located by means of proton bombardment of A^{40} and observation of an anomaly in the elastic scattering places this level at a proton energy of 908 kev. (± 10 kev.)

(2) The feasibility of using a proportional counter to observe anomalies in the elastic scattering of a gas has been demonstrated.

(3) Elastic scattering in A^{40} at energies between 710 and 1133 kev. and at a laboratory scattering angle of 150° follows closely that predicted from a computation of the differential cross-sections due to superposition of Coulomb scattering and scattering from an impenetrable sphere.

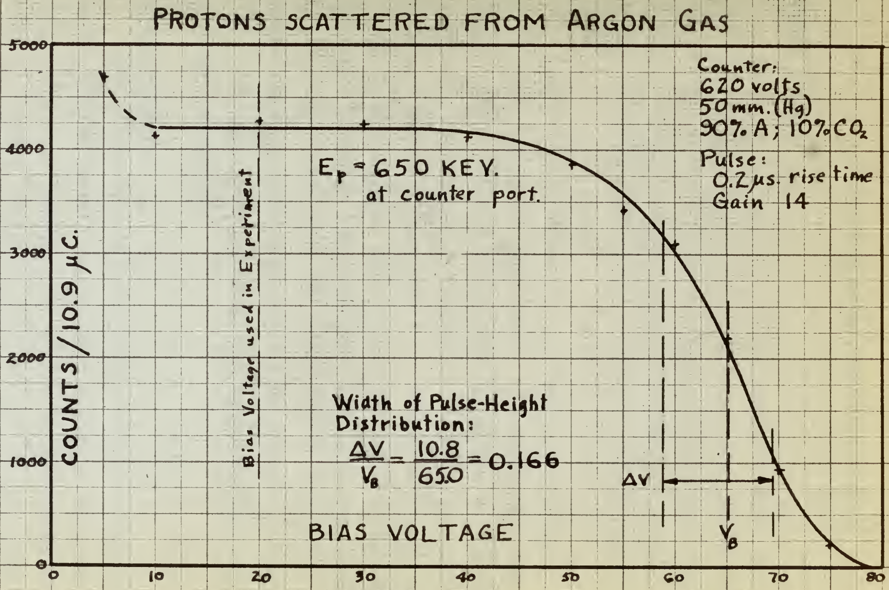
PROTONS SCATTERED FROM ARGON GAS

FIGURE 13.

VI. SUGGESTIONS FOR FUTURE EXPERIMENTS

Solid Targets.

As stated in Section I, one of the difficulties of using the present apparatus for solid targets is that visual observation of the beam is obstructed and alignment is extremely difficult especially since the very core of the proton beam must pass through a collimator of only 0.1" diameter.

A slight modification can be made by constructing a movable mounting for a solid target on a small shaft inserted through the wall of the reaction chamber or Faraday cage, pieces (2) and (3) of Figure 5. A vacuum seal gland would, of course, be necessary to avoid loss of pressure or vacuum in the chamber. With this modification, a solid target could be mounted, the apparatus closed and evacuated, and with the target swung out of the line of sight, the beam could be visually monitored and the apparatus aligned. Then, the target could be swung back into the proper position for bombardment.

Gaseous Targets.

With the use of a thin mica window over the entry port of the counting chamber, it would be possible to have one gas mixture in the proportional counter and another in the reaction chamber. Naturally, separate gas filling connec-

and a vacuum connection would have to be incorporated for the reaction chamber since it would be isolated from the counting chamber which now carries the gas filling connections and vacuum connection.

With this modification it would be possible to observe scattering and particle resonance reactions in different gases while still keeping the counting gas the same.

VII. TABLES

TABLE I

Discriminator Curve on Po^{210} Internal Source.

Pressure 200 mm. Hg.
Central Wire Voltage, +800 volts.
Rise time, 0.2 microseconds.
Using Model 205-B Preamplifier.
Amplifier Gain, 2.

Discriminator Bias Voltage	Alphas Counts per minute
2	218
5	201
10	144
15	148
20	136
25	138
30	136
32	135
35	135
38	92
40	58
42	30
44	4
46	1
48	0

TABLE II

EXPERIMENTAL MEASUREMENTS

Nickel Window to Reaction Volume:

Minimum	1.30 cm.
Maximum	2.33 cm.
Mean	1.82 cm.

Reaction Volume to Sensitive Volume of Proportional Counter:

Minimum	9.4 cm.
Maximum	10.4 cm.
Mean	9.9 cm.

Center of Target Volume to:

Near End of Sensitive Volume	9.9 cm.
Far End of Sensitive Volume	26.9 cm.

Length of Sensitive Volume:	17.0 cm.
Length of Reaction Collimator:	4.6 cm.
Diameter of Collimator Ports:	0.06" (0.152 cm.)
Thickness of Nickel Foil Window:	0.00005"(0.000127 cm.)
Laboratory Scattering Angle:	150° ± 1.9°
Diameter of Beam Aperture:	0.1" (2.54 mm.)
Width of Beam Slit:	1 mm.

TABLE III

Computation of Reaction Energy of Protons (E_m)

E_{beam} (kev.)	900	1000	1100	1200
E_{foil} (kev.)	745	855	963	1070
Range at foil (cm.)	1.65	2.03	2.43	2.86
ΔR_1 (1.03cm.)	.08	.08	.08	.08
R_1 (cm.)	1.57	1.95	2.35	2.78
ΔR_2 (2.33 cm.)	.15	.15	.15	.15
R_2 (cm.)	1.50	1.88	2.28	2.71
E_1 (kev.)	718	830	940	1050
E_2 (kev.)	696	812	922	1033
ΔE (kev.)	22	18	18	17
ΔR_m (1.82 cm.)	.12	.12	.12	.12
R_m (cm.)	1.53	1.91	2.31	2.74
E_m (kev.)	706	820	931	1042

$\Delta R_{1,2}$ are minimum and maximum thickness of gas in chamber at 50 mm. (Hg) pressure reduced to equivalent range at 760 mm.

Values of E_{foil} are plotted as Curve I in Figure 10.

Values of E_m are plotted as Curve II in Figure 10.

TABLE IV.

Energies of Elastically Scattered Protons at Entry Port of Counter (E_c)

E_b (kev.)	900	1000	1100	1200
E_m (Table III)	706	820	931	1042
E_r (E_m x 0.975)	689	800	909	1018
R_r (cm.)	1.47	1.83	2.22	2.64
ΔR_1 (9.4 cm.)	.62	.62	.62	.62
R_1 (cm.)	.85	1.21	1.60	2.02
ΔR_2 (10.4 cm.)	.68	.68	.68	.68
R_2 (cm.)	.79	1.15	1.54	1.95
E_1 (kev.)	465	601	730	853
E_2 (kev.)	440	568	707	830
ΔE (kev.)	25	24	23	23
ΔR_c (9.9 cm.)	.65	.65	.65	.65
R_c (cm.)	.82	1.18	1.57	1.99
E_c (kev.)	452	593	720	842

$\Delta R_{1,2}$ are minimum and maximum distance from target to entry port of counter reduced to 760 mm (Hg) pressure as in Table III.

Values of E_c are plotted as Curve III in Figure 10.

TABLE V

Theoretical No. of Scattered Protons into Solid Angle of 1/3144 at an Angle of 150°

E (Mev.)	0.700	0.800	0.900	1.000	1.100
E ($\times 10^{6}$ ergs)	1.12	1.28	1.44	1.60	1.76
v ($\times 10^{-9}$ cm/s)	1.17	1.25	1.33	1.40	1.47
λ ($\times 10^{12}$ cm)	3.46	3.24	3.04	2.89	2.76
$\frac{2\pi A}{\lambda}$ (rad.)	.932	.994	1.060	1.114	1.167
$\frac{2\pi A}{\lambda}$ (degrees)	53.6°	56.95°	60.75°	63.8°	66.9°
$\sin^2(\frac{2\pi A}{\lambda})$	.644	.702	.761	.805	.846
$\frac{\lambda^2}{\pi}$ (barns)	3.82	3.35	2.95	2.66	2.43
σ_p (barns)	2.46	2.34	2.26	2.14	2.05
σ_c (barns)	.99	.75	.60	.48	.40
σ (barns)	3.45	3.09	3.86	2.62	2.45
$n(\Theta)$	4820	4320	4000	3670	3430

$$\sigma_p = \frac{\lambda^2}{\pi} \sin^2\left(\frac{2\pi A}{\lambda}\right)$$

$$\sigma_c = \left[\frac{zZe^2}{2\mu v}\right]^2 \frac{1}{\sin^4\left(\frac{\Theta}{2}\right)}$$

$$\sigma = \sigma_p + \sigma_c$$

$$n(\Theta) = n_o N t \sigma / 3144$$

$t = 0.366$ cm.

$n_o = 6.80 \times 10^{13}$ protons/10.9 uC.

$N = 1.77 \times 10^{17}$ atoms/cc.

TABLE VI

Discriminator Data on Scattered Protons.

E_o = 650 kev. at counter port. Counter pressure, 50 mm (Hg).

Counter voltage, +620 volts

Gas: 90% A; 10% - CO_2

Rise time, 0.2 μsec.

Amplifier Gain, 14

Bias Voltage	Counts/ 10.9 nC.
5	4697
10	4132
20	4271
30	4240
40	4122
50	3851
55	3402
60	3100
65	2199
70	938
75	247
80	8

REFERENCES

1. Born. Z. Physik **38**, 803 (1926). Also Landé. *Quantum Mechanics*, p.94, Pitman Pub. Corp. (1951).
2. Dicke and Marshal. Phys. Rev. **63**, 86 (1943).
3. Wilkins. Phys. Rev. **60**, 365 (1941).
4. Davis and Hafner. Phys. Rev. **73**, 1242 (1948).
5. Powell, May, Chadwick, and Pickavance. Nature **145**, 893 (1940).
6. Fulbright and Bush. Phys. Rev. **74**, 1323 (1948).
7. Rhoderick. Proc. Roy. Soc. London A, **201**, 348 (1950).
8. Rutherford, Chadwick, and Ellis. *Radiations from Radioactive Substances*. (1930). Also Semat. *Atomic Physics* Rinehart (1946).
9. Crockfort and Walton. Nature **129**, 649 (1932).
10. Oliphant, Kempton, and Rutherford. Proc. Roy. Soc. **149**, 406 (1935).
11. Neuert. Phys. Zeit. **36**, 629 (1935).
12. Kirchner and Neuert. Phys. Zeit. **36**, 54 (1935).
13. Oliphant, Kempton, and Rutherford. Proc. Roy. Soc. **150**, 241 (1935).
14. Dee and Gilbert. Proc. Roy. Soc. **154**, 279 (1936).
15. Henderson, Livingston, and Lawrence. Phys. Rev. **46**, 38 (1934).
16. Halliday. *Introductory Nuclear Physics.* Wiley (1950).
17. Hornyak, Lauritsen, Morrison, and Fowler. Rev. Mod. Phys. **22**, 291, (1950).

18. Allburger, and Hafner. *The Properties of Atomic Nuclei.* Brookhaven National Laboratory Pamphlet BNL-T-9 (1949).

19. Devons. *Excited States of Nuclei.* Cambridge Press. (1949).

20. Freeman and Baxter. Nature *162*, 696 (1948).

21. Brostrøm, Huus, and Koch. Nature 162, 695 (1948).

22. Landé. *Quantum Mechanics.* Pitman (1951).

23. Wentzel. Z. Physik *40*, 590 (1926).

24. Siri. *Isotopic Tracers and Nuclear Radiations.* McGraw-Hill (1940).

25. Feshbach, Peaslee, and Weiskopf. Phys. Rev. *71*, 145 (1947).

26. Orear, Rosenfeld, Schluter. *Nuclear Physics.* Notes on a course given by Enrico Fermi. (1950).

27. Bethe. Rev. Mod. Phys. *9*, 69 (1937).

28. Rose. Phys. Rev. *57*, 958 (1940).

29. Bender, Shoemaker, Kaufmann, and Bouricius, Phys. Rev. *76*, 273 (1949).

30. Mooring, Koester, Goldberg, Saxon, and Kaufmann. Phy. Rev. *84*, 703 (Nov. 15, 1951).

31. Laubenstein and Laubenstein. Phys. Rev. *84*, 18 (1951)

32. Koester. Phys. Rev. *85*, 643 (Feb. 15, 1952).

33. A. B. Chilton. Master's Thesis. *The Design and Construction of an Apparatus for Detection of Proton-Alpha Nuclear Reactions.* Ohio State University.(1951)

34. W. E. L. Boyce. Master's Thesis. *A Current Integrator.* Ohio State University. (1952).

35. Hirschfelder and Magee. Phys. Rev. *73*, 207 (1948).

36. Madsen and Venkateswarlu. Phys. Rev. *74*, 1782 (1948).

MAY 20 871
JUN 3 871
JUN 9 876
MY 1 57 4638

17236
Thesis
D66

Dorsett

Investigation of proton induced reactions in light nuclei using proportional counter.

Thesis
D66
17236

Dorsett

Investigation of proton induced reactions in light nuclei using proportional counter.

ACCOPRESS BINDER
No. BG 2507 EMBOSSED
ACCO PRODUCTS INCORPORATED

thesD66missing
Investigation of proton induced reaction
3 2768 002 00611 6
DUDLEY KNOX LIBRARY